Stabilization of dense metallic Pb monolayer by decorating step edges with Au atoms on Si(111)

Jonathan Baptista, Sergio Vlaic, Enrico Cofler, Dimitri Roditchev, Stéphane Pons

Stabilization of dense metallic Pb monolayer by decorating step edges with Au atoms on Si(111)

Jonathan Baptista[a], Sergio Vlaic[a], Enrico Cofler[a], Dimitri Roditchev[a,b], Stéphane Pons[a,*]

[a]*Laboratoire de Physique et d'Étude des Matériaux, ESPCI Paris, Université PSL, CNRS UMR8213, Sorbonne Université, 75005 Paris, France*
[b]*Institut des Nanosciences de Paris, Sorbonne Université, CNRS UMR7588, 75005 Paris, France*

Abstract

Under specific conditions, the sequential growth of Au and Pb on Si(111) results in a huge modification of the surface structure which neither Au/Si nor Pb/Si growths provoke separately. Initially atomically flat 7x7 Si(111) substrate breaks into a terraced-hill structure containing up to 10 atomic terraces of a typical width 10-50 nm. Terraces are covered by a dense monolayer of Pb (nominal coverage 1.2 to 1.33 ML); their step edges are decorated by double rows of Au atoms. This opens a route for constructing superconducting Josephson devices on atomic scale.

Keywords: Lead, gold, silicon, monolayer, surface relaxation and reconstruction, surface structure, morphology, roughness and topography, scanning tunneling microscopy, Gundlach oscillation

1. Introduction

A very rich collection of ground states was discovered in single atomic metal layers at the surface of semiconductors, such as Mott transition [1, 2], Charge and Spin Density Waves[3], ordered magnetic phases[4, 5], 1D-physics[6], superconductivity[7, 8, 9]. These orders, often competing, are only recently accessible with states-of-the-art computations, and there are major discrepancies between experiments and theory for many systems. Single layers of metal atoms on semiconductors with strong spin-orbit

*Corresponding author
Email address: stephane.pons@espci.fr (Stéphane Pons)

interactions (e.g.[10, 11]) are also good candidates for Topological Mott Insulators[12] if they are combined to strong correlations. Remarkably, the phenomenon of superconductivity, evidenced in 2010 in single dense atomic layers of Pb/Si(111), was completely unexpected from the theoretical point of view[7]. Recent experiments on Pb/Si(111) show that the superconductivity develops at the very interface of Pb and Si and is not directly related to the superconducting nature of Pb bulk material[9].

Therefore, there is a current interest in understanding the parameters driving the emergence of new ordered phases in single layers of metals on silicon. It would open the way towards electronic-phase engineering, and make possible to disentangle the effects of superconductivity, electron-electron correlations and spin-orbit interactions. To this end, it can be anticipated that ordered alloys at the surface of silicon based on various alloying of chemical elements can yield new phases. For example, monolayers of Pb/Si(111) are known to produce superconductivity[7, 9] and some Au/Si(111) reconstructions[13] show strong Rashba spin-orbit interactions. It is rational to try to mix these properties in an alloy which could benefit of both properties. In this context we present a structural study of successive depositions of Au and Pb in the monolayer range on the surface of Si(111).

2. Experimental details

Samples were prepared under ultra-high vacuum (base pressure 1.10^{-10} mbar) before their in-situ studies in the scanning tunneling microscope (STM) held at 1.3 K. At this temperature Pb, Au and Si atoms diffusion is frozen. Bias voltage refers to the sample voltage with respect to the STM tip.

Before Au deposition the silicon surface was prepared by repeated direct current heating cycles consisting of flashes at 1150 °C. The last flashes were followed by slow cooling through the 7×7 reconstruction phase transition (3K per second). The preparation procedure was repeated until the silicon sample was exhibiting large terraces of 7×7 reconstruction with an antiphase chevron pattern for neighboring step edges. Sequential and simultaneous Pb and Au depositions were achieved. We obtained the results presented here when performing Au followed by Pb deposition. Gold was de-

posited by molecular beam epitaxy (MBE) at a rate of 0.2 ML per minute on the silicon substrate held at room temperature (RT). The samples were post-annealed 2 minutes at 580 °C by means of radiative heating. 5×2 crystallographic order was checked by LEED and STM. The 5×2 reconstruction was found to cover the full surface at nominal coverage of around 0.6 ML Au on Si(111). Pb deposition was performed by MBE on the 5×2 Au surface held at RT and then annealed at 420 °C by means of radiative heating. This temperature was already reported for inducing a slow evaporation of Pb from the surface and the production of well-organized reconstructions of Pb/Si(111)[14]. This temperature is too low for bulk migration or evaporation of Au atoms[15]. Depending on the Pb coverage and annealing time we obtained various structures which are detailed in the following.

3. results and discussion

5×2 *Au/Si(111) patterned surface as a template.* The 5×2 reconstructed Au/Si(111) surface was used as a template for further growth of a Pb dense monolayer. 5×2 Au/Si(111) is composed of parallel chains of gold atoms siting on the silicon surface separated by gaps of naked silicon[16, 17, 18, 19, 20] which produce the peculiar topography pattern presented figure1. It has been proposed that Si adatoms are expelled form the substrate when the reconstruction takes place. One can expect a concentration of Si adatoms variation from 0.025 to 0.05 ML[21, 22, 23]. These adatoms occupy randomly a given adsorption site on top of the Au atomic chains[21, 22]. It is still unclear if the Si adatoms play a role for the stabilization of the structure but we have also observed the presence of these adatoms, as visible in the inset of figure 1. For low coverage the surface shows already domains of 5×2 Au/Si(111) separated by clean 7×7 Si(111) regions as we show in figure 1 for 0.25 ML of Au. Our sample preparation parameters yield the nucleation of the 5×2 at the top edge of the steps and domain propagation at the upper part of the terraces. The 5×2 domains show 3 orientations and are well faceted. They also appear to be elongated in one direction. Far from the step edges (>50 nm), some 5×2 domains also nucleate. In between the 5×2 domains bare silicon 7×7 reconstruction was seen to remain intact. We

have found that the full coverage of the surface occurs for 0.5 to 0.6 ML in agreement with previous experimental works[16, 17, 18]. The fully covered surface shows defects presented figure 2 which are important for the following Pb growth. The orientational domains are seen to be elongated in the direction of the Au chains. For our deposition parameters, the domains are of around $150 \times 50\,\mathrm{nm}^2$ in agreement with the distance between reconstruction nucleus found in figure 1. The orientation of the domains are not related to step edge orientation. The domain boundaries can be decorated by an accumulation of atomic defects probably composed of an excess of Si or Au adatoms at twin boundaries. Phase slips or stacking faults are seen at boundaries of neighboring domains of same orientation. The excess of Si adatoms can coalesce into silicon islands which are then covered by the 5×2 reconstruction. Some of these islands nucleate at step edges on the bottom terrace and form protrusions. The protrusions are seen to be smaller than the typical domains lying on the original silicon terraces. As the step edges are not anymore as regular as the bare silicon ones and exhibit protrusions, we can conclude that the underlying silicon terraces can be remodeled by Au adsorption.

Short annealing of Pb-Au on silicon : the "leopard" domains. Before we analyze the deposition of Pb on Au/Si(111) let's consider the case of pure Pb on Si(111). Pb/Si(111) is known to be capable to accept extremely large variation of stress, the atomic density of Pb can vary of more than a factor of 4 from the dilute to the ultra-compact dense phase locally showing structural buckling. In between, the well established phases corresponding to the $\alpha - \sqrt{3} \times \sqrt{3}$ R30 °, with a coverage ratio (θ) of $\frac{1}{3}$ ML and $\beta - \sqrt{3} \times \sqrt{3}$ R30 ° with a coverage of $\frac{4}{3}$ ML, Pb/Si(111) shows at least 15 macroscopically developed crystallographic phases[24, 25, 26, 27, 28, 29, 30, 31, 32, 33, 14] which vary one from the other of less than a percent of a ML, this phenomenon is know as the devil's staircase[34]. Various phases with very similar Pb density (corresponding to nominal coverage of 1.20 to $\frac{4}{3}$ML of pure Pb) were found on the surface of our samples (see below). These phases, i.e. stripe (SIC), hexagonal (HIC) incommensurate and linear phases[35] have been found metallic and even superconducting[7, 8, 9] at 1K.

The deposition of 1.1 ML of Pb on 5×2-Au/Si(111) followed by a post annealing at

420 °C for 2 minutes produced the sample shown in figure 3. Two kinds of domains are visible, the first one appearing darker in the topography image occupies approximately 70% of the surface and is composed of Pb-SIC phase. The other one covers around 30% of the surface and corresponds to less organized patches connected to step edges. The latter domains are referred here as "leopard domains". When the step edges are faceted they are decorated by a sharp bright lines. It seems that the surface kept the memory of the 5×2-Au domains since the sample shows similar domain boundaries with lines of accumulated defects. Some vacancy islands nucleate at these reminiscent domain boundaries which are used as pit-holes for Si extraction as shown in the following.

The atomically resolved image presented in figure 4 confirms the presence of SIC-Pb domains. In contrast, the crystallographic ordering of the leopard domains is not well-defined although short distance ordering exists. Terrace height corresponds to the distance between successive Si(111) planes in agreement with the monolayer nature of Pb and leopard domains standing on a silicon plane. The bright lines at step edges appear to be composed of 2 rows. The width of each row, approximately 1.75 nm, may indicate that each row are composed of more than line of one atoms. The appearing height of these lines is different than the one of Si and Pb atoms; it will be referred as "double rows" in the following. This step termination seems to be very well connected to the leopard domains (see profiles in figure 4). Moreover the height of the leopard domains is very similar to the one of the double rows at step edges. This last point is in agreement with a growth of the double-row at the upper step edge. The new phase does not seem to have a long-range order and, for Pb on silicon, neither such a phase was observed nor any step termination of this kind. figure 5 shows an interesting configuration. A silicon island covered by the leopard domains appears at the center of the image. The double-row of atoms is under construction at the upper part of the step where the Pb-SIC order in the lower terrace is not perturbed, indicating that the Pb atoms in the vicinity of the step edge are not involved in the growth of the double-row but only the atoms of the leopard domains. The growth of the double rows is seen to be accompanied with the faceting of the islands which are irregular elsewhere. In figure 5, it is also shown that the double rows can protrude from the terraces leaving the Pb covered terrace irregular as undetermined adatoms start to accumulate around

this protrusion. Such double rows were not evidenced in pure Pb/Si(111) samples.

For all these reasons and since these features were not observed previously in Pb/Si(111) systems, we attribute the double rows to Au chains with single or most probably double layer thickness at step edges. As a corollary, leopard domains consist of Au-rich phase possibly alloyed with Pb and Si. The total density of the metal atoms deposited at surface is surprising because it is much higher than the one of Pb observed phases and Au 5 monolayers. This disagreement is understood when analyzing SEM images of the surface, shown in figure 7 where micronic and submicronic nanocrystals are seen to lye on the Pb-Au/Si(111) flat surface indicating that the excess of Au and Pb atoms can be stocked in 3D nanocrystals of pure or mixed chemical composition.

Decorated dense Pb phases. A longer annealing at 420 °C ($\approx$ 15 minutes) yields a very corrugated but perfectly ordered surfaces, see figure 6. The following discussion is also valid for larger deposited amount of Pb (we have made experiments with up to 5 ML). The terraces are fully covered by coexisting HIC, SIC and linear phases of Pb/Si(111). Each step edge is decorated by the double rows of Au atoms. On the topographic image of figure 6, which is relevant for almost all the surface (see the discussion of the SEM image bellow), one can count at least 10 different atomic levels on a surface of $150 \times 150\,\mathrm{nm}^2$ whereas the average distance between two successive steps for the silicon substrate before deposition was estimated to be of the order of 120 nm with a dominant downward slope with positive X direction. So, the silicon underlying step structure has been deeply and completely remodeled by the deposition. This is in agreement with figure 5 where the double rows formation produces faceted step edges and where vacancy islands are observed.

A mapping of 93×93 Z(V) spectra was used for determining the surface electronic homogeneity liked to the chemical composition of the area presented in figure 8, where typical surface structures are found, including a Pb nanocrystal used as a reference (Pb composition was established by measuring the STS superconducting gap in conductance spectra not shown here). The result of $\left.\frac{dZ(V)}{dV}\right|_I$ spectra over various regions is presented in figure 8b) and c). These spectra show well pronounced Gundlach[36] oscillations which are the consequence of resonant tunneling conductance between the

tip and the surface in the field effect regime through the vacuum levels in the barrier. The characteristic voltages oscillations are dependent on the density of states of the surface and also to the tunneling barrier shape. Any effect of the local variation of the work function and/or of the dielectric constant yields strong modification of the the conductance and so of the spectra. As a result any spatial distribution of the total charge density, electrostatic potential or electron affinity (in a more chemical picture) at atomic scale which bends the potential barrier at the surface involves a modification of the Gundlach osciations[37]. So, the experiment tells us first, if we put aside the Pb nanocrystal and the double rows at step edge, that the surface is terminated by a similar structure of the same chemical elements(i.e no Pb-Au alloy on the terrace), as expected for the homogeneity of the Pb covered terraces. The homogeneity of the Gundlach oscillations tells us also that the coupling of the wave functions of the bulks states of the sample and the vacuum states inside the STM junction is everywhere on the reconstructed terraces the same. This last observation rules out the hypothesis of different Pb thicknesses in the sample. So our sample consists of dense Pb monolayers decorated Au double rows lying on a very corrugated silicon substrate. It means that the presence of Au in the system produces a deep reorganization of the substrate and the growth of terraced-hill like pyramids of Si.

4. Conclusion

In conclusion we have shown that the growth of Pb on 5×2 Au/Si(111) induces a strong reorganization of the silicon substrate and a demixing of Pb and Au. Pb recovers the terraces and organizes in hexagonal, stripe incommensurate and linear phases where gold builds double rows of atoms at step edges. We suggest that the gold decoration of step edges is enough energetically favorable for being the driving force of the pyramid creation since it was shown that Au covering is able to expel silicon adatoms from the substrate and also that the double rows are shown to facet the terraces. Once the balance between the line energy at step edges, the surface energy of the Pb covered terraces and the elastic energy is reach the excess of Au and Pb atoms is stocked in big nanocrystals. This growth mechanism is shown to stabilize a Pb density of the order

of 1.2 to 1.33 ML where Pb/Si(111) is superconducting at low temperature[7, 8, 9]. In this context, the Au decorated steps could behave as atomically controlled Josephson junctions useful for further device fabrication.

5. Acknowledgements

The PhD grant of J. B. is supported by the Labex Matisse and the Nexans Chair through the PhaseOnSi project. We thank the French national research agency for the support of the SUPERSTRIPES project, Re. ANR-15-CE30-0026.

6. Bibliography styles

References

References

[1] S. Modesti, L. Petaccia, G. Ceballos, I. Vobornik, G. Panaccione, G. Rossi, L. Ottaviano, R. Larciprete, S. Lizzit, A. Goldoni, Insulating ground state of $\mathrm{Sn/Si(111)}-(\sqrt{3}\times\sqrt{3})r30^{\circ}$, Phys. Rev. Lett. 98 (2007) 126401. doi:10.1103/PhysRevLett.98.126401.
URL https://link.aps.org/doi/10.1103/PhysRevLett.98.126401

[2] P. Hansmann, T. Ayral, L. Vaugier, P. Werner, S. Biermann, Long-range coulomb interactions in surface systems: A first-principles description within self-consistently combined gw and dynamical mean-field theory, Phys. Rev. Lett. 110 (2013) 166401. doi:10.1103/PhysRevLett.110.166401.
URL https://link.aps.org/doi/10.1103/PhysRevLett.110.166401

[3] J. M. Carpinelli, H. H. Weitering, M. Bartkowiak, R. Stumpf, E. W. Plummer, Surface charge ordering transition: α phase of sn/ge(111), Phys. Rev. Lett. 79 (1997) 2859–2862. doi:10.1103/PhysRevLett.79.2859.
URL https://link.aps.org/doi/10.1103/PhysRevLett.79.2859

[4] G. Li, P. Höpfner, J. Schäfer, C. Blumenstein, S. Meyer, A. Bostwick, E. Rotenberg, R. Claessen, W. Hanke, Magnetic order in a frustrated two-dimensional atom lattice at a semiconductor surface, Nature Communications 4 (1) (2013) 1620. doi:10.1038/ncomms2617.
URL https://doi.org/10.1038/ncomms2617

[5] J.-H. Lee, H.-J. Kim, J.-H. Cho, Ferrimagnetic slater insulator phase of the Sn/Ge(111) surface, Phys. Rev. Lett. 111 (2013) 106403. doi:10.1103/PhysRevLett.111.106403.
URL https://link.aps.org/doi/10.1103/PhysRevLett.111.106403

[6] C. Blumenstein, J. Schäfer, S. Mietke, S. Meyer, A. Dollinger, M. Lochner, X. Y. Cui, L. Patthey, R. Matzdorf, R. Claessen, Atomically controlled quantum chains hosting a tomonaga–luttinger liquid, Nature Physics 7 (10) (2011) 776–780. doi:10.1038/nphys2051.
URL https://doi.org/10.1038/nphys2051

[7] T. Zhang, P. Cheng, W.-J. Li, Y.-J. Sun, G. Wang, X.-G. Zhu, K. He, L. Wang, X. Ma, X. Chen, Y. Wang, Y. Liu, H.-Q. Lin, J.-F. Jia, Q.-K. Xue, Superconductivity in one-atomic-layer metal films grown on Si(111), Nature Physics 6 (2) (2010) 104–108. doi:10.1038/nphys1499.
URL https://doi.org/10.1038/nphys1499

[8] M. Yamada, T. Hirahara, S. Hasegawa, Magnetoresistance measurements of a superconducting surface state of in-induced and pb-induced structures on si(111), Phys. Rev. Lett. 110 (2013) 237001. doi:10.1103/PhysRevLett.110.237001.
URL https://link.aps.org/doi/10.1103/PhysRevLett.110.237001

[9] C. Brun, T. Cren, V. Cherkez, F. Debontridder, S. Pons, D. Fokin, M. C. Tringides, S. Bozhko, L. B. Ioffe, B. L. Altshuler, D. Roditchev, Remarkable effects of disorder on superconductivity of single atomic layers of lead on silicon, Nature Physics

10 (6) (2014) 444–450. doi:10.1038/nphys2937.
URL https://doi.org/10.1038/nphys2937

[10] E. Frantzeskakis, S. Pons, M. Grioni, Band structure scenario for the giant spin-orbit splitting observed at the bi/si(111) interface, Phys. Rev. B 82 (2010) 085440. doi:10.1103/PhysRevB.82.085440.
URL https://link.aps.org/doi/10.1103/PhysRevB.82.085440

[11] I. Gierz, T. Suzuki, E. Frantzeskakis, S. Pons, S. Ostanin, A. Ernst, J. Henk, M. Grioni, K. Kern, C. R. Ast, Silicon surface with giant spin splitting, Phys. Rev. Lett. 103 (2009) 046803. doi:10.1103/PhysRevLett.103.046803.
URL https://link.aps.org/doi/10.1103/PhysRevLett.103.046803

[12] D. Pesin, L. Balents, Mott physics and band topology in materials with strong spin–orbit interaction, Nature Physics 6 (5) (2010) 376–381. doi:10.1038/nphys1606.
URL https://doi.org/10.1038/nphys1606

[13] I. Barke, F. Zheng, T. K. Rügheimer, F. J. Himpsel, Experimental evidence for spin-split bands in a one-dimensional chain structure, Phys. Rev. Lett. 97 (2006) 226405. doi:10.1103/PhysRevLett.97.226405.
URL https://link.aps.org/doi/10.1103/PhysRevLett.97.226405

[14] E. Ganz, F. Xiong, I.-S. Hwang, J. Golovchenko, Submonolayer phases of Pb on Si(111), Physical Review B 43 (9) (1991) 7316–7319. doi:10.1103/physrevb.43.7316.
URL https://link.aps.org/doi/10.1103/physrevb.43.7316

[15] N. Stolwijk, B. Schuster, J. Hölzl, H. Mehrer, W. Frank, Diffusion and solubility of gold in silicon, Physica B+C 116 (1) (1983) 335 – 342. doi:https://doi.org/10.1016/0378-4363(83)90271-1.

URL http://www.sciencedirect.com/science/article/pii/0378436383902711

[16] I. Barke, F. Zheng, S. Bockenhauer, K. Sell, V. v. Oeynhausen, K. H. Meiwes-Broer, S. C. Erwin, F. J. Himpsel, Coverage-dependent faceting of au chains on si(557), Phys. Rev. B 79 (2009) 155301. doi:10.1103/PhysRevB.79.155301.
URL https://link.aps.org/doi/10.1103/PhysRevB.79.155301

[17] McAlinden, N., McGilp, J. F., New evidence for the influence of step morphology on the formation of au atomic chains on vicinal si(111) surfaces, EPL 92 (6) (2010) 67008. doi:10.1209/0295-5075/92/67008.
URL https://doi.org/10.1209/0295-5075/92/67008

[18] J. Kautz, M. W. Copel, M. S. Gordon, R. M. Tromp, S. J. van der Molen, Titration of submonolayer au growth on si(111), Physical Review B 89 (3). doi:10.1103/physrevb.89.035416.
URL https://link.aps.org/doi/10.1103/physrevb.89.035416

[19] S. G. Kwon, M. H. Kang, Identification of the au coverage and structure of the $\mathrm{Au/Si(111)}-(5 \times 2)$ surface, Phys. Rev. Lett. 113 (2014) 086101. doi:10.1103/PhysRevLett.113.086101.
URL https://link.aps.org/doi/10.1103/PhysRevLett.113.086101

[20] S. C. Erwin, I. Barke, F. J. Himpsel, Structure and energetics of $\mathrm{Si(111)}-(5 \times 2)$-Au, Phys. Rev. B 80 (2009) 155409. doi:10.1103/PhysRevB.80.155409.
URL https://link.aps.org/doi/10.1103/PhysRevB.80.155409

[21] R. Bennewitz, J. N. Crain, A. Kirakosian, J.-L. Lin, J. L. McChesney, D. Y. Petrovykh, F. J. Himpsel, Atomic scale memory at a silicon surface, Nanotechnology

13 (4) (2002) 499–502. doi:10.1088/0957-4484/13/4/312.
URL https://doi.org/10.1088%2F0957-4484%2F13%2F4%2F312

[22] A. Kirakosian, J. Crain, J.-L. Lin, J. McChesney, D. Petrovykh, F. Himpsel, R. Bennewitz, Silicon adatoms on the si(111)52–au surface, Surface Science 532-535 (2003) 928 – 933, proceedings of the 7th International Conference on Nanometer-Scale Science and Technology and the 21st European Conference on Surface Science. doi:https://doi.org/10.1016/S0039-6028(03)00097-9.
URL http://www.sciencedirect.com/science/article/pii/S0039602803000979

[23] C. H. Patterson, S. Banerjee, J. F. McGilp, Reflectance anisotropy spectroscopy of the $\mathrm{Si}(111)-(5\times 2)\mathrm{Au}$ surface, Phys. Rev. B 94 (2016) 165417. doi:10.1103/PhysRevB.94.165417.
URL https://link.aps.org/doi/10.1103/PhysRevB.94.165417

[24] C. Kumpf, O. Bunk, J. H. Zeysing, M. M. Nielsen, M. Nielsen, R. L. Johnson, R. Feidenhans'l, Structural study of the commensurate–incommensurate low-temperature phase transition of pb on si(111), Surface Science 448 (2) (2000) L213 – L219. doi:https://doi.org/10.1016/S0039-6028(99)01224-8.
URL http://www.sciencedirect.com/science/article/pii/S0039602899012248

[25] M. Hupalo, T. L. Chan, C. Z. Wang, K. M. Ho, M. C. Tringides, Atomic models, domain-wall arrangement, and electronic structure of the dense $\mathrm{Pb/Si}(111)-\sqrt{3}\times\sqrt{3}$ phase, Phys. Rev. B 66 (2002) 161410. doi:10.1103/PhysRevB.66.161410.
URL https://link.aps.org/doi/10.1103/PhysRevB.66.161410

[26] B. Ressel, J. Slezák, K. C. Prince, V. Cháb, Quantized valence states

of the pb/si(111) mosaic phase, Phys. Rev. B 66 (2002) 035325. doi:10.1103/PhysRevB.66.035325.
URL https://link.aps.org/doi/10.1103/PhysRevB.66.035325

[27] T.-L. Chan, C. Z. Wang, M. Hupalo, M. C. Tringides, Z.-Y. Lu, K. M. Ho, First-principles studies of structures and stabilities of pb/si(111), Phys. Rev. B 68 (2003) 045410. doi:10.1103/PhysRevB.68.045410.
URL https://link.aps.org/doi/10.1103/PhysRevB.68.045410

[28] M. Yakes, V. Yeh, M. Hupalo, M. C. Tringides, Self-organization at finite temperatures of the devil's staircase in pb/si(111), Phys. Rev. B 69 (2004) 224103. doi:10.1103/PhysRevB.69.224103.
URL https://link.aps.org/doi/10.1103/PhysRevB.69.224103

[29] V. Yeh, M. Yakes, M. Hupalo, M. Tringides, Low temperature formation of numerous phases in pb/si(111), Surface Science 562 (1) (2004) L238 – L244. doi:https://doi.org/10.1016/j.susc.2004.05.133.
URL http://www.sciencedirect.com/science/article/pii/S0039602804006806

[30] S. Stepanovsky, M. Yakes, V. Yeh, M. Hupalo, M. Tringides, The dense -33pb/si(111) phase: A comprehensive stm and spa-leed study of ordering, phase transitions and interactions, Surface Science 600 (7) (2006) 1417 – 1430. doi:https://doi.org/10.1016/j.susc.2005.12.041.
URL http://www.sciencedirect.com/science/article/pii/S003960280501383X

[31] E. Ganz, H. Ing-Shouh, X. Fulin, S. K. Theiss, J. Golovchenko, Growth and morphology of pb on si(111), Surface Science 257 (1) (1991) 259 – 273. doi:https://doi.org/10.1016/0039-6028(91)90797-V.

URL http://www.sciencedirect.com/science/article/pii/003960289190797V

[32] C. J. Karlsson, E. Landemark, Y.-C. Chao, R. I. G. Uhrberg, Photoemission study of the Si(111)-$\sqrt{3} \times \sqrt{3}$ -Pb mosaic phase: Observation of a large charge transfer, Physical Review B 45 (11) (1992) 6321–6324. doi:10.1103/physrevb.45.6321.

[33] J. Gómez-Rodríguez, J.-Y. Veuillen, R. Cinti, Scanning tunneling microscopy study of the si(111)-(3 3)-pb mosaic phase, Surface Science 377-379 (1997) 45 – 49, european Conference on Surface Science. doi:https://doi.org/10.1016/S0039-6028(97)01325-3.
URL http://www.sciencedirect.com/science/article/pii/S0039602897013253

[34] M. Hupalo, J. Schmalian, M. C. Tringides, "devil's staircase" inPb/si(111)ordered phases, Physical Review Letters 90 (21). doi:10.1103/physrevlett.90.216106.
URL https://link.aps.org/doi/10.1103/physrevlett.90.216106

[35] S. Stepanovsky, M. Yakes, V. Yeh, M. Hupalo, M. Tringides, The dense -33pb/si(111) phase: A comprehensive stm and spa-leed study of ordering, phase transitions and interactions, Surface Science 600 (7) (2006) 1417 – 1430. doi:https://doi.org/10.1016/j.susc.2005.12.041.
URL http://www.sciencedirect.com/science/article/pii/S003960280501383X

[36] K. Gundlach, Zur berechnung des tunnelstroms durch eine trapezförmige potentialstufe, Solid-State Electronics 9 (10) (1966) 949–957. doi:10.1016/0038-1101(66)90071-2.
URL http://dx.doi.org/10.1016/0038-1101(66)90071-2

[37] C. L. Lin, S. M. Lu, W. B. Su, H. T. Shih, B. F. Wu, Y. D. Yao, C. S. Chang, T. T. Tsong, Manifestation of work function difference

in high order gundlach oscillation, Phys. Rev. Lett. 99 (2007) 216103. doi:10.1103/PhysRevLett.99.216103.
URL https://link.aps.org/doi/10.1103/PhysRevLett.99.216103

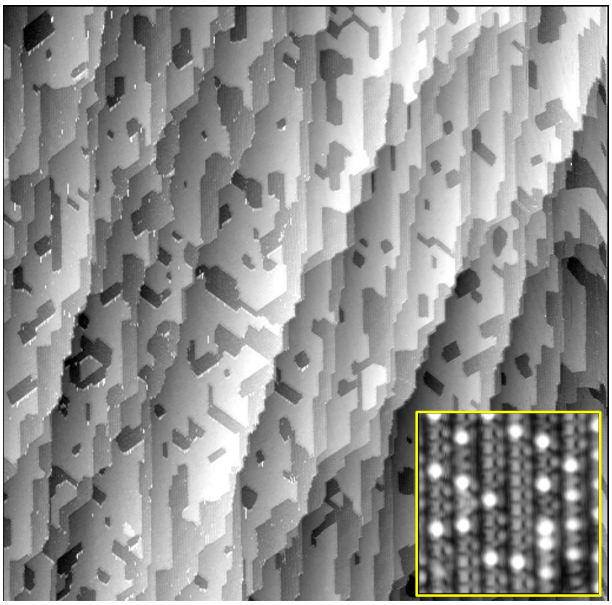

Figure 1: Au/Si(111): incomplete coeverage by 5x2 reconstruction. Topography image, $1000 \times 1000\,\mathrm{nm}^2$, ($V_{stab} = 1.0\,\mathrm{V}$ and $I_{stab} = 10\,\mathrm{pA}$) showing in a same step a bright reconstruction (7×7) and a dark ones (5×2). Inset: atomic resolution of a 5×2 domain showing Si adatoms adatoms on top of the Au rows. Image size: $10 \times 10\,\mathrm{nm}^2$. $V_{stab} = 1.0\,\mathrm{V}$ and $I_{stab} = 90\,\mathrm{pA}$).

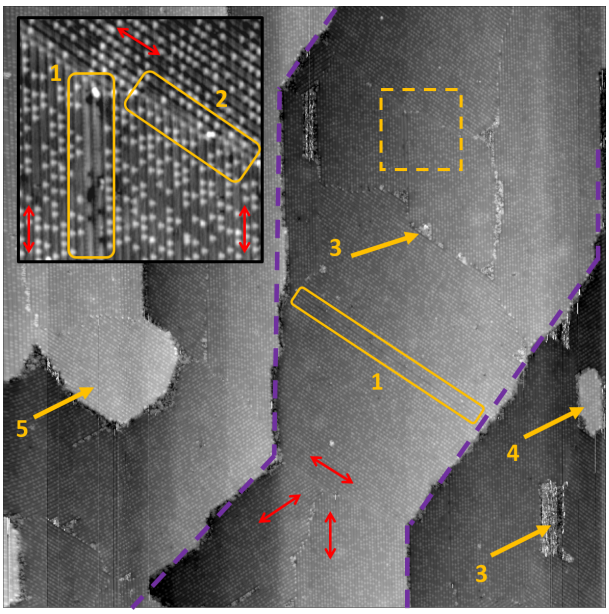

Figure 2: Scanning tunneling topography image of 5×2 Au/Si(111) at nominal coverage. The reconstruction orientation does not cross the step edges. The reminiscent silicon step can be recognized (dashed purple lines). Three orientational domains (oriented along red double-arrows) are separated by anti-phase (1) and twin (2) boundaries. The reconstruction produces a segregation of an excess of Si adatoms that are pushed at the domain boundaries (3) or redistributed in islands and protrusions of well organized islands (4 and 5). **inset** zoom on the region marked by a square. $V_{stab} = 1.0\,\mathrm{V}$ and $I_{stab} = 10\,\mathrm{pA}$. Size $300 \times 300\,\mathrm{nm}^2$.

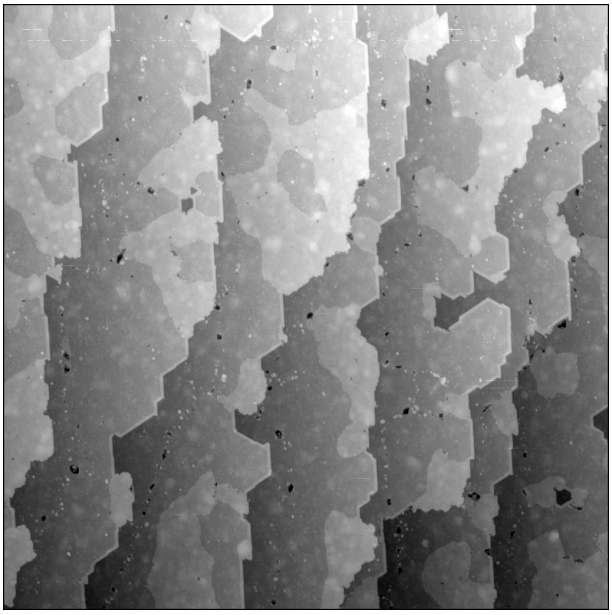

Figure 3: STM topography image of Pb deposited on Au/Si(111): Pb domains (dark) and leopard domains (bright) are coexisting on the surface. Image size: 500×500 nm^2. $V_{stab} = 1.0$ V and $I_{stab} = 5$ pA

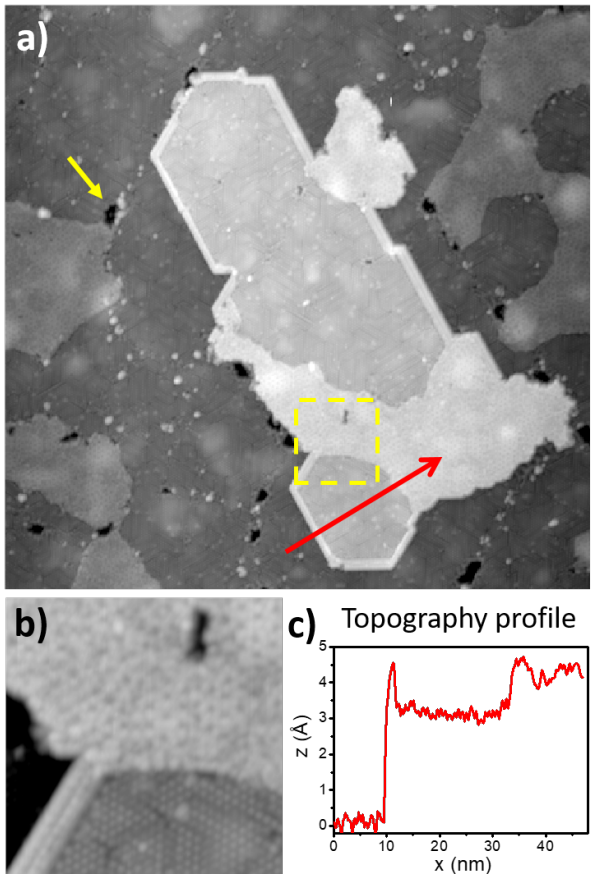

Figure 4: Pb deposition on 5×2 Au/Si(111) after short annealing. **a)** Topography image. $100 \times 100\,\mathrm{nm}^2$. The images shows that the surface corresponds to a patchwork of leopard domains and Pb domains. Some step edges are faceted and decorated by bright lines. An arrow points to one of the many vacancy islands nucleating at domain boundaries of the Pb and leopard domains. The dashed square corresponds to the zoomed image presented in b). **b)** An arrow show location of the profile presented in c). In **b)** atomic resolution image showing the presence of Pb incommensurate phase, and double rows of atoms connected to the leopard phase. Individual atoms cannot be resolved in the double rows. **c)** topography profile showing that the step height separating to Pb covered terraces corresponds to the silicon lattice parameter and that the leopard phase has the same height than the step decoration. $V_{stab} = 1.0\,\mathrm{V}$ and $I_{stab} = 10\,\mathrm{pA}$.

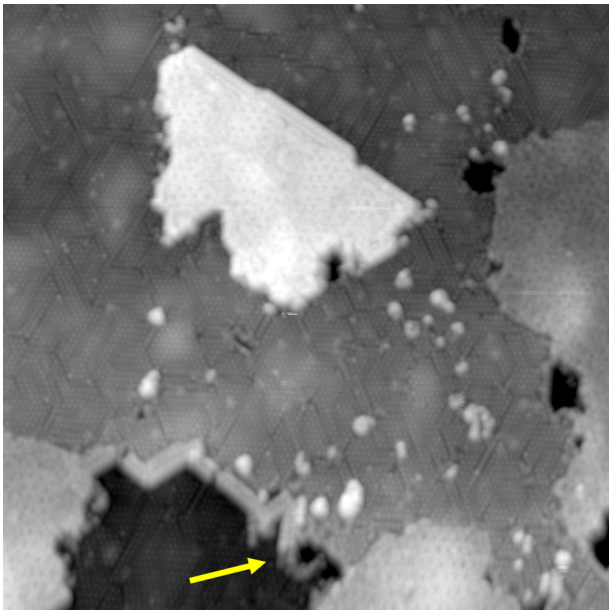

Figure 5: STM topography image showing the frozen double rows formation mechanism. The arrow points to double rows can protruding from the upper terrace. Image size: $80 \times 80\,\mathrm{nm}^2$. $V_{stab} = 1.0\,\mathrm{V}$ and $I_{stab} = 10\,\mathrm{pA}$.

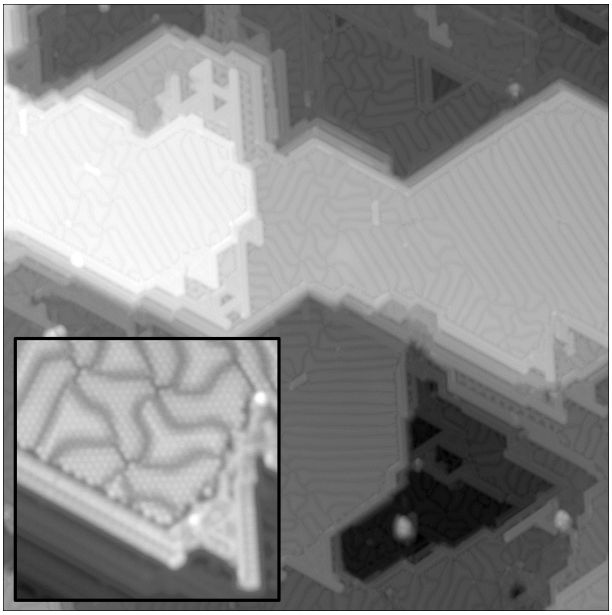

Figure 6: Pb+Au/Si(111): topography image of the decorated SIC phase 150×150 nm^2 $V_{stab} = 1.4$ V and $I_{stab} = 50$ pA, inset: zoom 16×16nm^2

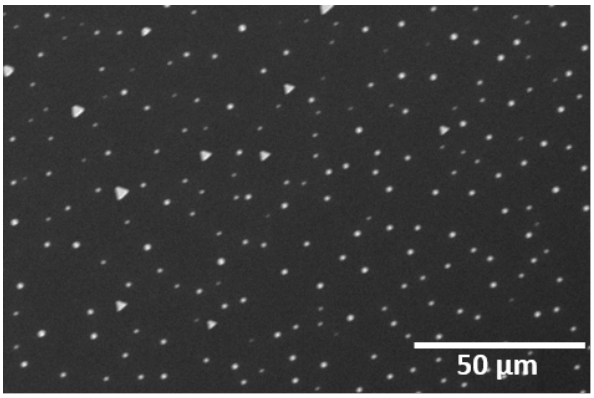

Figure 7: Pb+Au/Si(111): Scanning Electron Microscope image showing the presence of micronic crystals with triangular and hexagonal shapes.

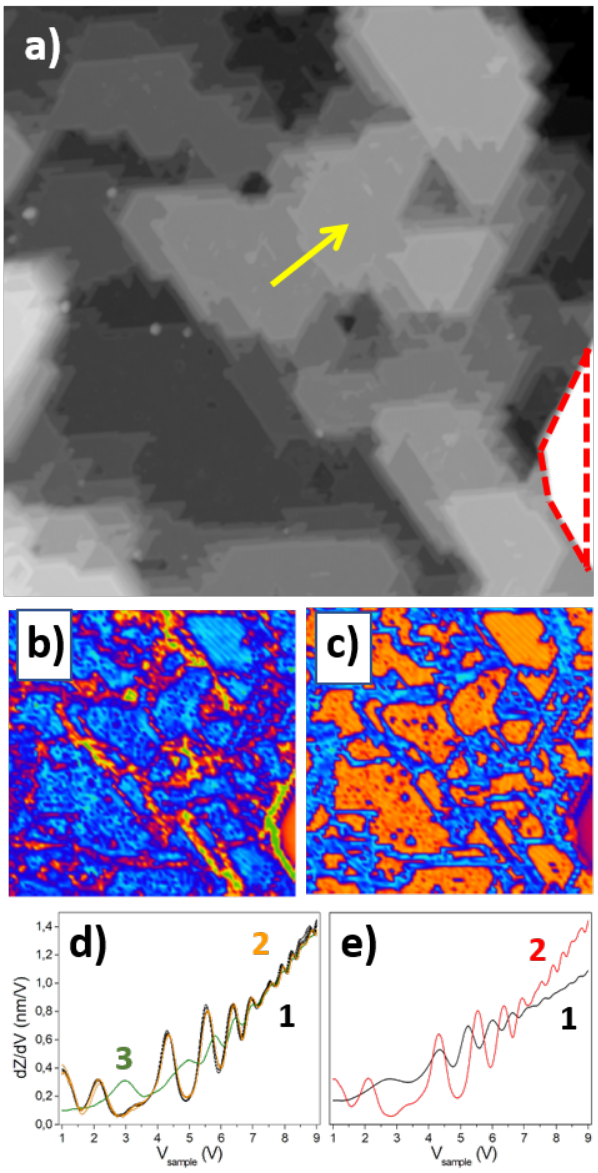

Figure 8: Metastable pyramidal strucutre of Pb-Au/Si(111). **a)** Topography image showing Pb covered terraces decorated by double rows of Au atoms. A Pb nanocrystal lye at the corner of the image delimited by a dashed red line. Image size: $340 \times 340\,nm^2$. $V_{stab} = 1.0\,\text{V}$ and $I_{stab} = 50\,\text{pA}$. The arrow shows the spatial distribution of the spectra presented in (d) **b)** and **c)** $\left.\frac{dZ(V)}{dV}\right|_I$ at 4.3 V and 6.6 V respectively showing the homogeneity of the chemical nature of Pb terraces, step edges and of the Pb nanocrystal. **d)** and **e)** $\left.\frac{dZ(V)}{dV}\right|_I$ spectra showing Gundlach Oscillations. d) $\left.\frac{dZ(V)}{dV}\right|_I$ spectra performed regularly taken along the arrow in figure a). Four spectra labeled (1) were taken on the lower terrace covered by Pb. Three Spectra labeled (2) were taken on the upper terrace covered by Pb. Spectrum labeled (3) corresponds to the decoration of the step edge by Au. Spectra (1) and (2) are almost identical indicating that successive Pb covered terraces have homogenous chemical properties. e) Averaged $\left.\frac{dZ(V)}{dV}\right|_I$ spectrum taken on the Pb nanocrystal (1) and averaged spectrum over all Pb covered terraces (2).